Journal of Interfaces, Thin films, and Low dimensional systems 7 (2) Winter and Spring (2024) 731-738

Controllable synthesis of ZnO nanorods supported by stainless steel mesh for photocatalytic degradation of organic pollutants

Scientific research paper

Yasaman Alaveh, Morasae Samadi*

Department of Physical Chemistry and Nanochemistry, Faculty of Chemistry, Alzahra University, Tehran, Iran

ARTICLE INFO

Article history:
Received 24 October 2023
Revised 13 December 2023
Accepted 16 December 2023
Available online 19 March 2024

Keywords
Semiconductor
Zinc oxide nanorods
Photocatalyst
Tetracycline
Methylene blue

ABSTRACT

In this research, zinc oxide (ZnO) nanorods were synthesized by the chemical bath deposition (CBD) method on steel mesh 400 for the photocatalytic decomposition of two organic pollutants: methylene blue (MB) dye and tetracycline (TC) antibiotic. Different parameters were studied, including the concentration of the nucleation solution, the number of deposition cycles, and the growth duration to reach the optimal state of ZnO nanorods growth. The optimal sample with a growth time of 3 h at a temperature of 95 °C and a concentration of 5 mM zinc acetate as a nucleation solution was used for photocatalytic degradation tests. The diffuse reflectance spectroscopy (DRS) analysis showed an energy gap of 3.2 eV for ZnO nanorods. The photodegradation rate constants were 0.0121 and 0.0043 min^{-1} for MB and TC removal, respectively. Also, the mechanism for the photocatalytic degradation was studied to propose the charge generation and transfer pathway.

1 Introduction

Currently, the increase in population in the world causes a further demand for the consumption of various drugs, including antibiotics. Different antibiotics are among the drugs that are used to prevent and treat bacterial infections [1]. The consumption dose of antibiotics and the introduction of many of these substances in municipal and hospital wastewater can lead to antibiotic residues in the water stream. It can induce severe problems such as mutation and cancer due to high stability and very low biodegradability, as well as antimicrobial resistance [2]. On the other hand, with the industrialization of societies and the increase in the number of industrial factories in the world, the amount of waste produced in this sector also increases. The effluents of these sections include materials such as heavy metals and dyes [3]. In the dyeing industry, more than half of the dyes enter the industrial wastewater directly without any change or hydrolysis, harming human health and aquatic ecosystems [4]. The weakness of common wastewater treatment in removing these organic materials as emerging pollutants (EPs) has encouraged the scientific community to apply newer and more effective methods [5, 6].

Considering the above-mentioned issues, one of the best and least expensive new water purification methods is the photocatalytic processes, which can decompose pollutants into less dangerous substances by producing active radicals [7]. Since 1972, many semiconductors have been utilized for photocatalytic degradation of organic pollutants, where ZnO and TiO_2 are among the widely used compounds in this field [8]. Zinc oxide nanomaterials have recently received more attention due to their light sensitivity, biocompatibility, chemical stability, suitable band gap, and high surface area.

*Corresponding author.
Email address: M.Samadi@alzahra.ac.ir
DOI: 10.22051/jitl.2023.45375.1098

[9,10]. One-dimensional (1D) ZnO nanorods have prominent growth along the c-axis direction, in which the surface energy is lower, and the surface area is higher; hence, this morphology is more favorable for the synthesis of ZnO than other structures for the photocatalytic applications [11,12]. Currently, recovery of the photocatalyst materials from the treated water via an easy and accessible method is desired. Therefore, using a chemically stable and non-toxic substrate for photocatalyst immobilization makes the recovery of the photocatalyst easy and inexpensive [13].

In this research, the steel mesh substrate, which has properties such as thermal stability, chemical stability, and flexibility, was used to grow zinc oxide nanorods by chemical method. Different synthesis parameters were changed to reach the optimum nanorod growth, and the sample was applied for photocatalytic degradation of two pollutants, namely methylene blue and tetracycline. Different charge carrier scavengers were utilized to elucidate the photodegradation pathway.

2 Materials and methods

2.1 Chemicals

Nitric acid (99% HNO_3), isopropyl alcohol (IPA 99%), zinc acetate, ethanol (99%), zinc nitrate, hexamethylenetetramine (HMTA), and polyethylene amine 750,000 (PEI) were purchased from Sigma-Aldrich. Tetracycline/HCl antibiotic and absolute ethanol were purchased from Hakim Pharmaceutical Company and Bidestan Company, respectively.

2.2 Synthesis of zinc oxide nanorods

First, a seed solution of 25 ml of zinc acetate solution in absolute ethanol with concentrations of 5, 0.5, and 0.05 M was prepared and then stirred for one hour at 60 °C by a magnetic stirrer and kept at room temperature for 24 h. Clean steel mesh was cut in sizes of 2.5 cm * 2 cm and put in seed solution by deep coating method with control of the immersion durations and times, namely 5 times for 2 min, 10 times for 2 min, and 10 times for 10 sec. Then, the steel mesh was baked for 15 minutes at 150 °C.

Table 1. Variables used in the synthesis of zinc oxide nanorods

Nucleation solution concentration	Immersion cycles	Growth time of nanorods
5 mM & 0.5 mM & 0.05 mM	10 times and 2 minutes each time & 5 times and 2 minutes each time & 10 times, and each time for 10 sec	3 & 6 h

2.3 Photocatalytic properties

To study the photocatalytic degradation of methylene blue dye (10^{-5} M) and tetracycline antibiotic (20 ppm), one steel mesh containing zinc oxide nanorods was placed in their 30 ml solution. Then, the solution was illuminated with a UV lamp with a power of 30 W and at a distance of 30 cm. The absorbance variations of methylene blue and tetracycline were checked at specific time intervals by UV-Vis spectroscopy. The maximum absorption peak for methylene blue and tetracycline was checked at 666 and 359 nm, respectively. To compare the rate of photocatalytic decomposition (k) of two samples, Eq. (1) was used [14]:

$$\mathrm{Ln}\frac{C_0}{C} = kt, \quad (1)$$

where k is the rate of photocatalytic decomposition, t is the time, C_0 is the initial solution concentration, and C is the concentration of the solution at different times.

2.4 Characterizations

Scanning electron microscopy (SEM) images were taken using the Vega3 LMU model produced by Tescan, Czech Republic. Diffusion reflectance spectroscopy (DRS) analysis was performed by Shimadzu UV-2600i ultraviolet spectrometer. UV-Vis spectra for photocatalytic degradation were performed by a Unico2150 device.

3 Results and discussion

The SEM images of the samples with different parameters are demonstrated in Tables 2, 3, and 4. As it is clear from the figures, changing the synthesizing parameters can lead to different morphologies. In Table 2, nucleation solution concentrations were changed, and the immersion cycles and growth time were constant.

Increasing the seed solution concentrations from 0.05 to 5 mM changed the density of the grown nanorods. The growth sites were not created at lower concentrations of the seed solution, so the nanorods did not grow. But at the concentration of 5 mM, the nanorods are arranged well and have a hexagonal structure. Therefore, the 5 mM concentration was selected for further experiments.

Table 3, compare immersion cycles' effect, including immersion times and durations. A comparison between different samples shows that the immersion of 10 times, each time for 2 minutes, can fabricate more density and population of ZnO nanorods. In this case, the growth centers are placed together entirely regularly, and a regular structure of nanorods was grown together. But, when the number of cycles decreases from 10 to 5 times, the number of growth centers is reduced and does not create a favorable structure. Also, 10 times, and each time for 10 sec for the immersion cycle, cannot lead to the formation of the nanorods. Therefore, the 10 times and 2 minutes immersion cycles was selected as an optimized condition.

The next factor is the duration of the growth phase of zinc oxide nanorods. Table 4 compares the SEM results for 3 and 6 h. Although, for 3 h growth time, the well-defined nanorods can be observed, a dense thin film was formed by the growth time of 6h. Other researchers reported the merging of the nanorods by increasing the growth time and the formation of thin film due to the lateral size growth of the nanorods. Therefore, the parameters that led to the synthesizing of Figure 1c were selected as the optimal parameters.

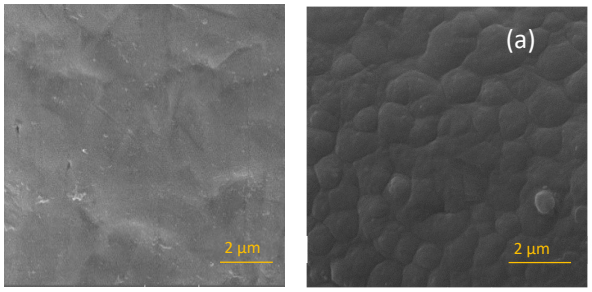

Figure 1. a) SEM images of the pure stainless-steel mesh and b) seed layer on the steel mesh with optimized parameters of 5mM of nucleation solution concentration and 10 times for 2 minutes each time as immersion cycle.

To compare the deposition of the nucleation sites for nanorods growth, SEM images of the pure steel mesh and deposited seed layer with optimized parameters are shown in Figure 1. The islands formed on the substrate in Figure 1b are the growth center for 1-dimensional growth of the ZnO.

Table 2. The effect of nucleation solution concentrations with other constant variables for ZnO nanorods growth.

SEM images	Nucleation solution concentration	Immersion cycles	Growth time of nanorods
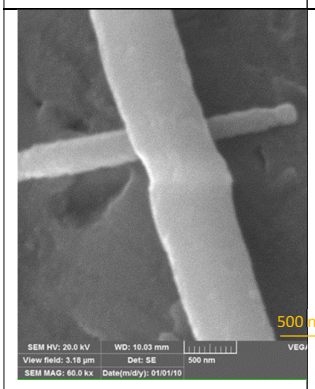	0.05 mM	10 times and 2 minutes each time	3 h
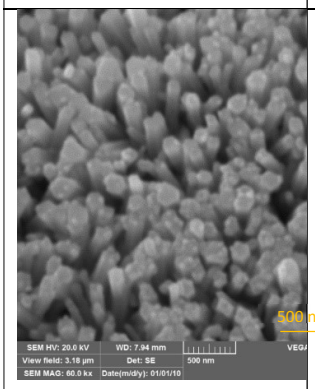	0.5 mM	10 times and 2 minutes each time	3 h
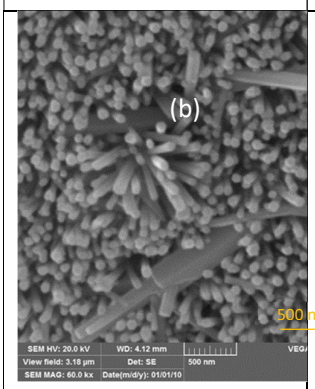	5 mM	10 times and 2 minutes each time	3 h

Table 3. The effect of immersion cycles with other constant variables for ZnO nanorods growth.

SEM images	Nucleation solution concentration	Immersion cycles	Growth time of nanorods
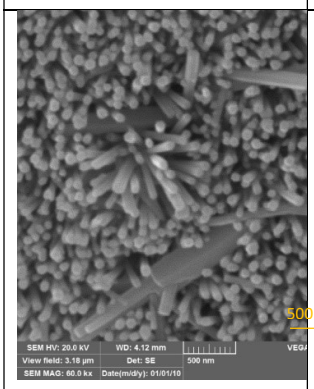	5 mM	10 times and 2 minutes each time	3 h
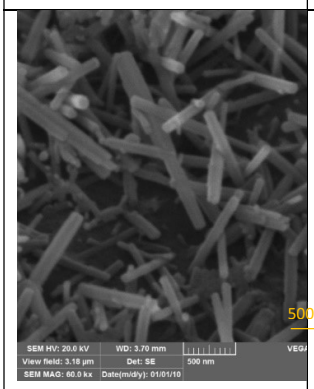	5 mM	5 times and 2 minutes each time	3 h
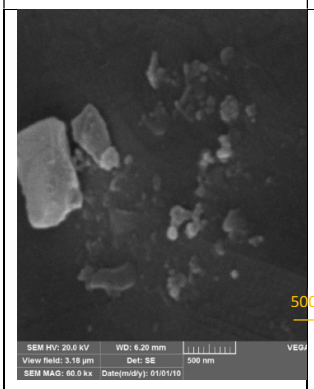	5 mM	10 times, and each time for 10 sec	3 h

Figure 2a shows the absorption spectrum obtained by DRS analysis of the optimal sample. The absorption edge of the synthesized nanorods is around 390 nm. Figure 2b shows graph $(ah\upsilon)^2$ vs. $h\upsilon$. Based on Eq. (2), by plotting a tangent line, the value of the energy gap of nanorods can be obtained [16].

$$ahv = K(hv - E_g)^{1/2}, \quad (2)$$

where a is the optical absorption coefficient, $h\upsilon$ is the incident photon energy, K is a constant number, and E_g is the band gap energy of the sample. The value of the energy gap obtained through the spectrum is about 3.2 eV, which is consistent with the values reported in the articles [17].

Table 4. The effect of growth time with other constant variables for ZnO nanorods growth.

SEM images	Nucleation solution concentration	Immersion cycles	Growth time of nanorods
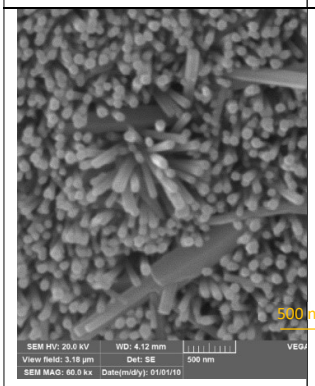	5 mM	10 times and 2 minutes each time	3 h
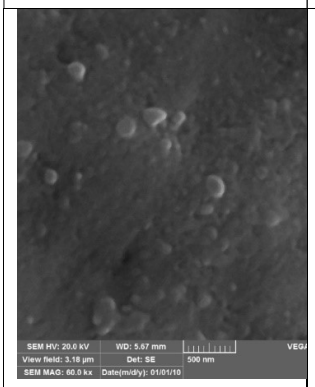	5 mM	10 times and 2 minutes each time	6 h

Figure 3 shows the XRD pattern of the optimal sample of zinc oxide nanorods. As shown in the figure, the characteristic peaks (101), (002), (100), (102), (103), (110), and (112) are related to the zinc oxide structure with the Wurtzite phase and hexagonal network structure. These values are consistent with those reported in the articles and with standard card JCPDS no.01-087-0713 [18].

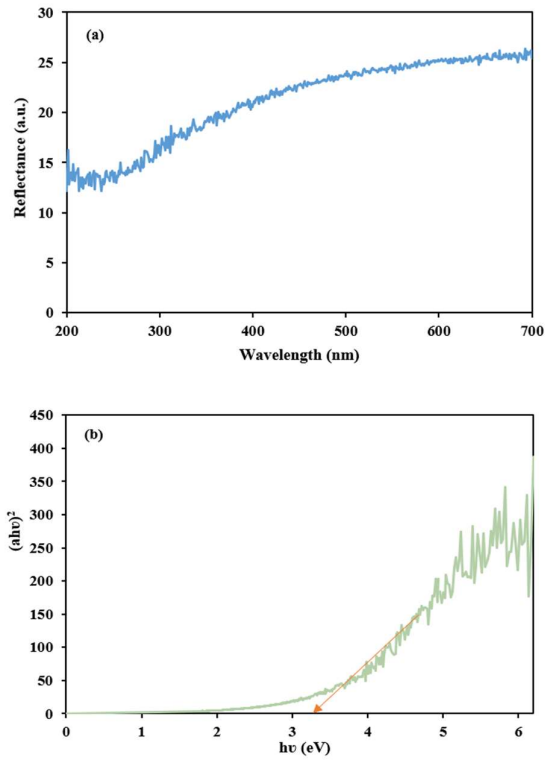

Figure 2. a) Reflection spectrum and b) diagram $(ah\upsilon)^2$ vs. $h\upsilon$ for ZnO nanorods on steel mesh

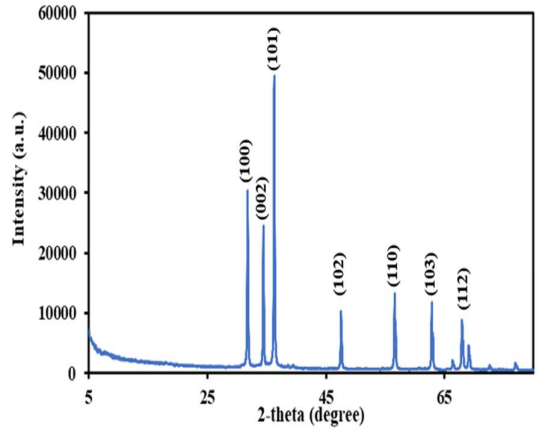

Figure 3. X-ray diffraction pattern of the optimal sample of zinc oxide nanorods.

Figure 4a shows the variation of methylene blue absorption during the photocatalytic degradation. It is evident that during light illumination, the concentration of methylene blue decreases due to photodegradation by the ZnO nanorods sample. Figure 4b illustrates $Ln(C_0/C)$ vs. time for photolysis (without using any photocatalyst) and ZnO nanorods sample. The degradation rate in photolysis and the presence of photocatalysts are 0.0006 and 0.0121 min^{-1}, respectively. Therefore, about 67% of methylene blue degrades after 90 min.

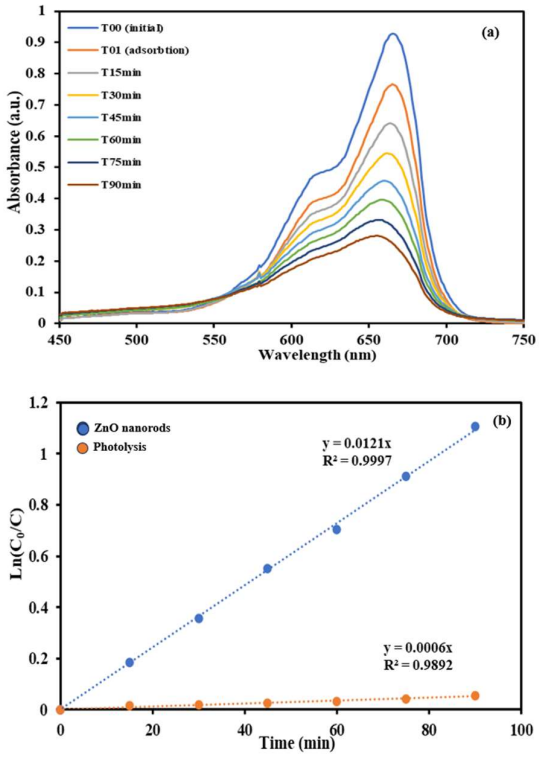

Figure 4. a) UV-Vis absorption spectrum of methylene blue in the presence of ZnO nanorods. b) LnC_0/C vs. time for ZnO nanorods and photolysis for methylene blue photodegradation under UV light illumination.

Figure 5a shows the decrease in the absorbance of tetracycline during the light illumination in the presence of the ZnO nanorods sample. Figure 5b illustrates $Ln(C_0/C)$ vs. time for photolysis and ZnO nanorods sample. The degradation rate in photolysis and the presence of photocatalysts are 0.0007 and 0.0043 min^{-1}, respectively. Therefore, the photodegradation is seven times greater than photolysis and about 32% of tetracycline degrades after 90 min.

To elucidate the mechanism of photocatalytic reaction on the surface of the ZnO nanorods, the influence of various charge carrier scavengers on the photodegradation efficiency of TC was studied under UV light irradiation. For this purpose, silver nitrate ($AgNO_3$) as an electron scavenger, Ethylenediaminetetraacetic acid (EDTA) as a hole scavenger, Isopropyl alcohol (IPA) as a hydroxyl radical (•OH) scavenger, and O_2 purging as a superoxide radical ($•O_2^-$) species scavenger were used.

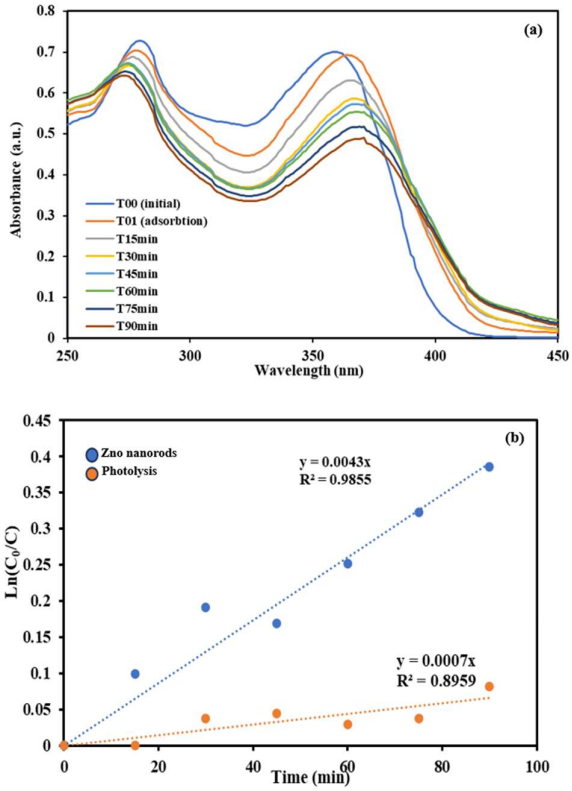

Figure 5. a) UV-Vis absorption spectrum of tetracycline in the presence of ZnO nanorods. b) LnC_0/C vs. time for ZnO nanorods and photolysis for tetracycline photodegradation under UV light illumination.

Figure 6 shows the rate of photodegradation of TC under UV light irradiation in the presence of different scavengers. A comparison of the k values demonstrated that eliminating electron, hole, and •OH via scavengers leads to enhanced photodegradation. O_2 is reduced compared to the condition without a scavenger. Photogenerated electrons scavenging increases the photodegradation because their recombination with holes retard, which can be the evidence of holes as a main pathway. Also, hole scavenger can reduce the electron-hole recombination; therefore, photogenerated electrons also play a crucial role in photodegradation. Purging O_2 decreases the photodegradation rate, which can be due to the increased interaction between the photogenerated electron and O_2. As the electrons are one of the main photodegradation pathways, therefore $•O_2^-$ production via electrons reduces the photocatalytic process efficiency. Based on these results, Figure 7 demonstrates that the generation of electrons in the conduction band and holes in the valence band cause the mineralization of TC molecules under UV light illumination.

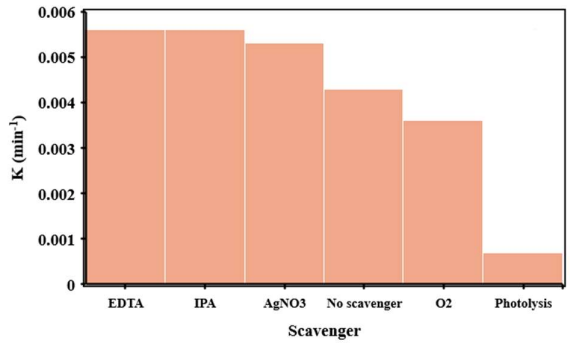

Figure 6. Degradation rate constants of TC on the ZnO nanorods in the presence of different scavengers and O_2 purging under UV irradiation.

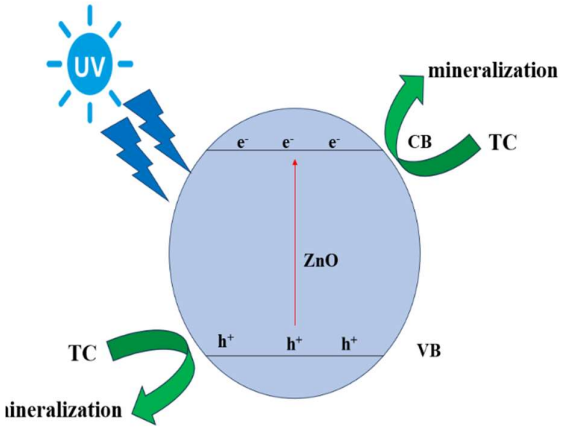

Figure 7. Proposed mechanism of charge transfer and photodegradation of TC on the surface of zinc oxide nanorods under UV light.

4 Conclusions

In this research, ZnO nanorods were synthesized on a steel mesh substrate with different factors such as concentration of seed solution, immersion cycles, and growth time. The higher concentration of the nucleation solution, i.e., 5 mM, was the best concentration to create the desired density and morphology of the ZnO nanorods. Based on the SEM images, the samples were prepared with 10 times each time for 2 min immersion, where the growth time for 3 h was the most appropriate condition for high-density ZnO nanorods. The photodegradation rates were studied, and the results showed that the photodegradation by ZnO nanorods for methylene blue and tetracycline are 20 and 7 times greater than photolysis, respectively. Photogenerated electrons and holes are the main pathways for

tetracycline antibiotic photodegradation. The flexibility and accessible synthesis of the mentioned photocatalyst and the fast recovery from the treated wastewater are promising for this photocatalyst's practical applications.

Acknowledgments

The authors thank Alzahra University for supporting this project.

References

[1] H. Wang et al., "Visible-light-driven removal of tetracycline antibiotics and reclamation of hydrogen energy from natural water matrices and wastewater by polymeric carbon nitride foam." Water Research, **144** (2018) 215.

[2] H. Al Abdulgader et al., "Hybrid ion exchange–Pressure driven membrane processes in water treatment: A review." Separation and Purification Technology, **116** (2013) 253.

[3] M. S. Mauter et al., "The role of nanotechnology in tackling global water challenges." Nature Sustainability, **1** (2018) 166.

[4] T. O. Durotoye et al., "Impact assessment of wastewater discharge from textile industry in Lagos, Nigeria." Cogent Engineering, **1** (2018) 1531687.

[5] Z. Hu et al., "Efficiency evaluation with feedback for regional water use and wastewater treatment." Journal of hydrology, **562** (2018) 703.

[6] M. Sheikh et al., "Application of ZnO nanostructures in ceramic and polymeric membranes for water and wastewater technologies: a review." Chemical Engineering Journal, **391** (2020) 123475.

[7] A. Monteoliva-García et al., "Effects of carrier addition on water quality and pharmaceutical removal capacity of a membrane bioreactor–advanced oxidation process combined treatment. Science of the Total Environment, **708** (2020): 135104.

[8] R. K. Upadhyay et al. "Role of graphene/metal oxide composites as photocatalysts, adsorbents and disinfectants in water treatment: a review." RSC Advances, **4** (2014) 3823.

[9] K. M. Lee et al., "Recent developments of zinc oxide based photocatalyst in water treatment technology: a review." Water Research, **88** (2016) 428.

[10] S. H. Chan et al., "Recent developments of metal oxide semiconductors as photocatalysts in advanced oxidation processes (AOPs) for treatment of dye waste-water." Journal of Chemical Technology & Biotechnology, **86** (2011) 1130.

[11] M. Samadi et al., "Recent progress on doped ZnO nanostructures for visible-light photocatalysis." Thin Solid Films, **605** (2016) 2.

[12] M. Samadi et al., "Design and tailoring of one-dimensional ZnO nanomaterials for photocatalytic degradation of organic dyes: a review." Research on Chemical Intermediates, **45** (2019) 2197.

[13] R. Molinari et al., R, Photocatalytic membrane reactors: Configurations, performance and applications in water treatment and chemical production, In Handbook of membrane reactors, Woodhead Publishing, (2013) 808-845.

[14] Y. Wang, "ZnO nanorods for gas sensors, in Nanorods and Nanocomposites." IntechOpen, (2020) 35-55.

[15] M. R. Almamari, Mohammed Rashid et al, "Some distinct attributes of ZnO nanorods arrays: Effects of varying hydrothermal growth time." Materials, **15** (2022) 5827.

[16] M. Samadi et al., "Synergism of oxygen vacancy and carbonaceous species on enhanced photocatalytic activity of electrospun ZnO-carbon nanofibers: Charge carrier scavengers mechanism." Applied Catalysis A: General, **466** (2013) 153.

[17] J. B. Coulter et al., "Assessing Tauc plot slope quantification: ZnO thin films as a model system." Physica Status Solidi (b), **255** (2018) 1700393.

[18] M. Samadi et al., "Visible light photocatalytic activity of novel MWCNT-doped ZnO electrospun nanofibers." Journal of Molecular Catalysis A: Chemical, **359** (2012) 42.